

# Numerical and Analytical study of Water Pollution Dynamics in a 3-D Aquatic Region using Diffusion-Advection Model

**Tarjani Naik, Mukesh Patel, Rachna Patel**

Ph.D. Scholar, Department of Mathematics, Uka Tarsadia University, Bardoli, Gujarat, India

Assistant Professor, Department of Mathematics, Uka Tarsadia University, Bardoli, Gujarat, India

Assistant Professor, Department of Computer Engineering, CGPIT, Uka Tarsadia University, Bardoli, Gujarat, India

tarju\_naik16@yahoo.com, mukesh.mt@gmail.com, rachu.cuty@gmail.com

---

## Abstract

### **Article History:**

**Received:** 28-06-2025

**Revised:** 20-08-2025

**Accepted:** 29-08-2025

Water pollution is a significant environmental issue that damage community health, aquatic life diversity, and the sustainable use of natural resources. Precise mathematical models are essential for representing and predicting pollutant movement in three-dimensional (3-D) water environments. This research introduces a 3-D diffusion-advection model aimed at examining the spatial and temporal fluctuations of pollution levels in aquatic systems. The aim is to describe the progressive accumulation of pollution in a 3-D space and to assess the efficiency of both analytical and numerical methods to addressed the diffusion-advection model. The analytical expression is obtained through the Adomian Decomposition Method (ADM), whereas the Du Fort–Frankel (DF) method serves as the numerical approach. The model employs initial and boundary conditions derived from experimented data (Exp. data) performed in a 3-D cuboid tank where water as a medium and an iodized salt water solution act as the pollutant. Pollution levels are assessed at various 3-D grid location within the tank over time to confirm the model's accuracy. The results obtained indicate a consistent rise in pollutant levels that align closely with both ADM and DF solutions. The insignificant variations, indicated in parts per million (PPM), emphasize the precision and dependability of the suggested model. In general, the combination of experimental findings with analytical and numerical methods creates a reliable foundation for studying pollutant dispersion in three-dimensional water systems. The study enhances modelling methods for diffusion–advection processes and offers important insights for water quality evaluation, environmental protection, and sustainable resource management.

**Keywords** Water pollution · 3-D Diffusion-Advection equation · Du Fort Frankel method · Adomian Decomposition method  
Mathematics Subject Classification 35K57· 65N06

---

## Introduction

Water is among the most vital resources on the Earth, covering almost two-thirds of its area. Freshwater is essential for human existence, and ensuring its adequate quantity and quality is an increasing worldwide issue [1, 2, 21]. Pollution of water sources from household and industrial practices poses a major issue in various areas, leading to approximately 25 million

dead each year due to the harmful impacts of polluted water [3, 4]. Consequently, water quality has emerged as a significant concern for the environment and public health. Water pollution happens when the physical, chemical, or biological properties of water change, scary for both aquatic environments and human health [1, 22]. These modifications are mainly caused by human actions, which undermine environmental management and public safety.

To deal with these issues, both analytical and numerical methods can be utilized to resolve mathematical models of water pollution. This research utilizes a 3-D diffusion-advection model to discover the spatial and temporal changes in pollutant concentration, taking into account diffusion and advection processes. Water serves as the medium, while a solution of iodized salt-water solution is utilized as the pollutant. The 3-D region of water tank is divided into evenly spaced grid locations, and data on pollutant concentration, recorded in parts per million (PPM), are gathered at each location over time. These observed Exp. data give the model's initial and boundary conditions. Two computational methods: the DF numerical method and the ADM for analytic solutions are employed to estimate pollutant concentrations. The outcomes are compared with Exp. data to assess precision and measure variation between the methods' results.

## 1 Related Work

A.K. Misra, J.B. Shukla, and Peeyush Chandra [6] explored the joint impact of saturation and water contamination on dissolved oxygen (DO) levels in aquatic ecosystems through mathematical models founded on differential equations. Zainab Yahya, Hanani Johari, and Nursalasawati Rusli [1] forecasted the movement of pollutants in water utilizing a one-dimensional (1-D) advection–diffusion model, addressed through Finite Difference Methods such as FTCS and the Implicit Crank–Nicolson approaches. Nigar Sultana and Laek Sazzad Andallah [7] utilized the second-order Lax–Wendroff method alongside the FTCS approach to address the 1-D advection–diffusion equation, calculating pollutant levels in rivers at different times and places. The 1-D advection–diffusion model was enhanced by Abbas Parsaie and Amir Hamzeh Haghiabi [12], alongside Safia Meddah, Omar Hireche, Mohamed Hadjel, and Abdelkader Saidane [13]. In [12], the model was employed to simulate contaminant spread in rivers through the Finite Volume Method and Artificial Neural Networks (ANN) to assess the longitudinal dispersion coefficient. In [13], the Transmission Line Matrix Method was utilized to find the highest pollutant concentration over a specified time frame and to assess longitudinal dispersion. Later research expanded the 1-D advection–diffusion model by adding more parameters, as shown by Delong Wan and Huiping Zeng [8], Nonparent Pochai, J.J.H. Miller, L.J. Crane, and Suwon Tangmanee [9], Tsegaye Simon and Purnachandra Rao Koya [10], as well as R.V. Waghmare and S.B. Kiwne [11]. The Pollution Index Method was utilized in [8] to forecast water quality based on various factors. In [9], the model evaluated expenses for water purification and determined pollutant concentrations through the Finite Element Method. The dynamics of river pollution were investigated in [10], using numerical solutions derived from the Splitting Method, Crank–Nicolson, and Runge–Kutta methods, where diffusion and reaction components were segregated and addressed separately. Analytical methods were utilized in [11] to obtain system solutions. C.A. Poffal, J.R. Zabadal, and S.B. Leite [5]

extended the study to a two-dimensional (2-D) advection-diffusion model, analyzing the distribution of materials and microorganisms in rivers and lakes through innovative iterative analytical method

## 2 Proposed Methodology

The proposed mathematical architecture for 3-D water pollution estimation is described as shown in Fig. 1.

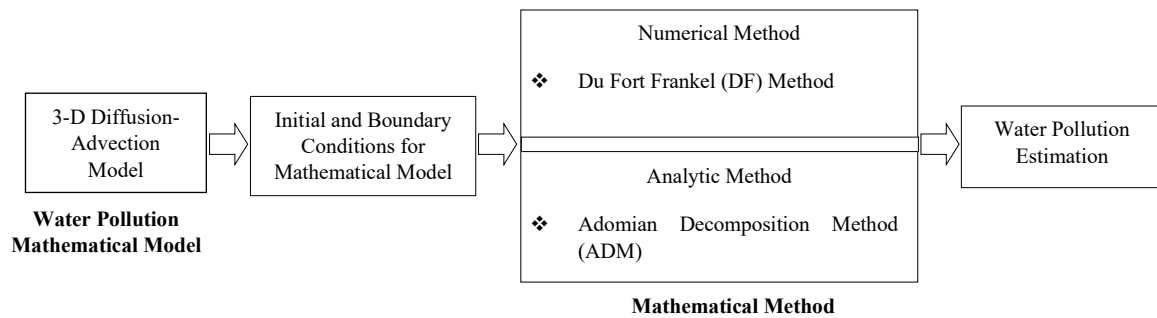


**Fig. 1** Mathematical architecture for 3-D water pollution estimation

### 2.1 Water Pollution Mathematical Model

The mathematical model for estimating water pollution is constructed based on the diffusion-advection model in 3-D region. The rate at which pollution concentration varies concerning time  $t$  at different 3-D location in  $x, y, z$  direction is mathematically formulated as in Eq. (1).

$$\frac{\partial w}{\partial t} = D \left( \frac{\partial^2 w}{\partial x^2} + \frac{\partial^2 w}{\partial y^2} + \frac{\partial^2 w}{\partial z^2} \right) - A \left( \frac{\partial w}{\partial x} + \frac{\partial w}{\partial y} + \frac{\partial w}{\partial z} \right) \quad (1)$$

where,  $t_0 \leq t \leq t_l, x_0 \leq x \leq x_r, y_0 \leq y \leq y_s, z_0 \leq z \leq z_p$  and the parameter  $w$  indicate the pollutant concentration along the  $x, y$  and  $z$  direction, while  $t$  refers to time,  $x, y$  and  $z$  represent directions,  $\frac{\partial^2 w}{\partial x^2}, \frac{\partial^2 w}{\partial y^2}, \frac{\partial^2 w}{\partial z^2}$  represent second ordered spatial derivative of concentration and  $\frac{\partial w}{\partial x}, \frac{\partial w}{\partial y}, \frac{\partial w}{\partial z}$  represent first ordered spatial derivative of concentration in all three directions. The diffusion rate  $D$  and advection rate  $A$  remains constant across all directions.

### 2.2 Initial and Boundary Conditions for Mathematical Model

The numerical and analytical solution  $w(x, y, z, t)$  of the mathematical model described in Eq. (1) is obtained by DF and ADM, respectively, which requires initial and boundary conditions concerning space and time. The initial conditions for time  $t$  are as in Eq. (2).

$$\left. \begin{aligned} w_0(x, y, z, t) &= w(x, y, z, t_0) = \phi_0(x, y, z) \\ w_1(x, y, z, t) &= w(x, y, z, t_1) = \phi_1(x, y, z) \end{aligned} \right\} \quad (2)$$

And boundary conditions for  $x, y$  and  $z$  directions are as in Eq. (3)

$$\left. \begin{aligned} w(x_0, y, z, t) &= \Psi_1(y, z, t) \\ w(x_r, y, z, t) &= \Psi_2(y, z, t) \\ w(x, y_0, z, t) &= \Psi_3(x, z, t) \\ w(x, y_s, z, t) &= \Psi_4(x, z, t) \\ w(x, y, z_0, t) &= \Psi_5(x, y, t) \\ w(x, y, z_p, t) &= \Psi_6(x, y, t) \end{aligned} \right\} \quad (3)$$

Where,  $\emptyset_0, \emptyset_1, \Psi_1, \Psi_2, \Psi_3, \Psi_4, \Psi_5$  and  $\Psi_6$  are known functions.

### 2.3 Mathematical Method

The diffusion-advection equation can be solved using various analytical and numerical techniques. This research utilizes the DF method to obtain numerical solutions and the ADM for the analytical approach.

#### 2.3.1 Du Fort Frankel Method (DF) [17, 18, 19]

The DF Method is a finite difference method used to get a numerical solution for the mathematical diffusion-advection model. The finite number of grid locations in  $x, y$  and  $z$  directions of 3-D regions at which the water pollution is estimated over a finite time interval is expressed as follows [20];

The grid points  $(x_a, y_b, z_c, t_d)$  are given as

$$\left. \begin{aligned} x_a &= x_0 : \delta x : x_r, & a &= 0, 1, 2, \dots r \\ y_b &= y_0 : \delta y : y_s, & b &= 0, 1, 2, \dots s \\ z_c &= z_0 : \delta z : z_p, & c &= 0, 1, 2, \dots p \\ t_d &= t_0 : \delta t : t_l, & d &= 0, 1, 2, \dots l \end{aligned} \right\} \quad (4)$$

in which  $r, s, p$  and  $l$  are integers and  $\delta x, \delta y$  and  $\delta z$  are grid spacing of all three directions respectively and  $\delta t$  is a time step size. We denote  $w(x_a, y_b, z_c, t_d) = w(x, y, z, t)$  in the finite difference approximation.

---

$\frac{\partial w}{\partial t} = \frac{w(x, y, z, t + 1) - w(x, y, z, t - 1)}{2\delta t}$	The central difference for time-space derivative (5)
---	--

$\frac{\partial^2 w}{\partial x^2} = \frac{w(x + 1, y, z, t) - 2w(x, y, z, t) + w(x - 1, y, z, t)}{\delta x^2}$	The spatial derivative's central difference in the $x$ direction (6)
---	--

$\frac{\partial^2 w}{\partial y^2} = \frac{w(x, y + 1, z, t) - 2w(x, y, z, t) + w(x, y - 1, z, t)}{\delta y^2}$	The spatial derivative's central difference in the $y$ direction (7)
---	--

$$\frac{\partial^2 w}{\partial z^2} = \frac{w(x, y, z + 1, t) - 2w(x, y, z, t) + w(x, y, z - 1, t)}{\delta z^2}$$

The spatial derivative's central difference in the z direction (8)

$$\frac{\partial w}{\partial x} = \frac{w(x + 1, y, z, t) - w(x - 1, y, z, t)}{2\delta x}$$

The central difference for first order derivative in x-direction on t time row (9)

$$\frac{\partial w}{\partial y} = \frac{w(x, y + 1, z, t) - w(x, y - 1, z, t)}{2\delta y}$$

The central difference for first order derivative in y-direction on t time row (10)

$$\frac{\partial w}{\partial z} = \frac{w(x, y, z + 1, t) - w(x, y, z - 1, t)}{2\delta z}$$

The central difference for first order derivative in z-direction on t time row (11)

Applying Eq. (5) - (11) in Eq. (1),

$$\begin{aligned} \frac{w(x,y,z,t+1)-w(x,y,z,t-1)}{2\delta t} = & D \left[ \frac{w(x+1,y,z,t)-2w(x,y,z,t)+w(x-1,y,z,t)}{\delta x^2} + \right. \\ & \left. \frac{w(x,y+1,z,t)-2w(x,y,z,t)+w(x,y-1,z,t)}{\delta y^2} + \frac{w(x,y,z+1,t)-2w(x,y,z,t)+w(x,y,z-1,t)}{\delta z^2} \right] - \\ & A \left[ \frac{w(x+1,y,z,t)-w(x-1,y,z,t)}{2\delta x} + \frac{w(x,y+1,z,t)-w(x,y-1,z,t)}{2\delta y} + \frac{w(x,y,z+1,t)-w(x,y,z-1,t)}{2\delta z} \right] \end{aligned}$$

(12)

Consider the same grid spacing in Eq. (12) for all three directions that  $\delta x = \delta y = \delta z = \delta$ .

$$\begin{aligned} w(x, y, z, t + 1) - w(x, y, z, t - 1) = & \frac{2 * D * \delta t}{\delta^2} [w(x + 1, y, z, t) + w(x - 1, y, z, t) + \\ & w(x, y + 1, z, t) + w(x, y - 1, z, t) + w(x, y, z + 1, t) + w(x, y, z - 1, t) - \\ & 6w(x, y, z, t)] - \frac{A * \delta t}{\delta} [w(x + 1, y, z, t) - w(x - 1, y, z, t) + w(x, y + 1, z, t) - \\ & w(x, y - 1, z, t) + w(x, y, z + 1, t) - w(x, y, z - 1, t)] \end{aligned}$$

(13)

Letting  $\frac{D * \delta t}{\delta^2} = \mu$  and  $\frac{A * \delta t}{\delta} = \eta$  in Eq. (13),

$$\begin{aligned} w(x, y, z, t + 1) = & w(x, y, z, t - 1) + 2\mu[w(x + 1, y, z, t) + w(x - 1, y, z, t) + \\ & w(x, y + 1, z, t) + w(x, y - 1, z, t) + w(x, y, z + 1, t) + w(x, y, z - 1, t) - \\ & 6w(x, y, z, t)] - \eta [w(x + 1, y, z, t) - w(x - 1, y, z, t) + w(x, y + 1, z, t) - \\ & w(x, y - 1, z, t) + w(x, y, z + 1, t) - w(x, y, z - 1, t)] \end{aligned}$$

(14)

Now, replace  $w(x, y, z, t)$  by the mean of the values  $w(x, y, z, t + 1)$  and  $w(x, y, z, t - 1)$

i.e.  $w(x, y, z, t) = \frac{w(x, y, z, t+1) + w(x, y, z, t-1)}{2}$  in Eq. (14),

$$w(x, y, z, t + 1) = w(x, y, z, t - 1) + 2\mu \left[ w(x + 1, y, z, t) + w(x - 1, y, z, t) + w(x, y + 1, z, t) + w(x, y - 1, z, t) + w(x, y, z + 1, t) + w(x, y, z - 1, t) - 6 \left( \frac{w(x, y, z, t+1) + w(x, y, z, t-1)}{2} \right) \right] - \eta [w(x + 1, y, z, t) - w(x - 1, y, z, t) + w(x, y + 1, z, t) - w(x, y - 1, z, t) + w(x, y, z + 1, t) - w(x, y, z - 1, t)]$$

$$(1 + 6\mu) w(x, y, z, t + 1) = (1 - 6\mu) w(x, y, z, t - 1) + 2\mu [w(x + 1, y, z, t) + w(x - 1, y, z, t) + w(x, y + 1, z, t) + w(x, y - 1, z, t) + w(x, y, z + 1, t) + w(x, y, z - 1, t)] - \eta [w(x + 1, y, z, t) - w(x - 1, y, z, t) + w(x, y + 1, z, t) - w(x, y - 1, z, t) + w(x, y, z + 1, t) - w(x, y, z - 1, t)]$$

Therefore, the following finite difference formula is used by the DF method to solve the 3-D diffusion-advection Eq. (1):

$$w(x, y, z, t + 1) = \frac{(1-6\mu)}{(1+6\mu)} w(x, y, z, t - 1) + \frac{2\mu}{(1+6\mu)} [w(x + 1, y, z, t) + w(x - 1, y, z, t) + w(x, y + 1, z, t) + w(x, y - 1, z, t) + w(x, y, z + 1, t) + w(x, y, z - 1, t)] - \frac{\eta}{(1+6\mu)} [w(x + 1, y, z, t) - w(x - 1, y, z, t) + w(x, y + 1, z, t) - w(x, y - 1, z, t) + w(x, y, z + 1, t) - w(x, y, z - 1, t)] \quad (15)$$

This Eq. (15) is the explicit formula of the DF method, and here, finding the solution at the  $t + 1$  level, requires the solution at some location of  $t$  level and  $t - 1$  level. Therefore, this method requires two initial conditions, shown in Eq. (2).

### 2.3.2 Adomian Decomposition Method (ADM) [14, 15, 16, 24]

In ADM method, re-write Eq. (1) in the standard operator form as

$$L_t w = D (L_{xx} w + L_{yy} w + L_{zz} w) - A (L_x w + L_y w + L_z w) \quad (16)$$

where,  $L_t = \frac{\partial}{\partial t}$ ,  $L_{xx} = \frac{\partial^2}{\partial x^2}$ ,  $L_{yy} = \frac{\partial^2}{\partial y^2}$ ,  $L_{zz} = \frac{\partial^2}{\partial z^2}$ ,  $L_x = \frac{\partial}{\partial x}$ ,  $L_y = \frac{\partial}{\partial y}$  and  $L_z = \frac{\partial}{\partial z}$ .

Taking the inverse operator of the operator  $L_t$  exists and it defined as

$$L_t^{-1}(\cdot) = \int_0^t (\cdot) dt$$

Thus, applying the inverse operator  $L_t^{-1}$  to Eq. (16) yields

$$\begin{aligned} L_t^{-1} L_t w(x, y, z, t) &= D (L_t^{-1} L_{xx} w + L_t^{-1} L_{yy} w + L_t^{-1} L_{zz} w) \\ &- A (L_t^{-1} L_x w + L_t^{-1} L_y w + L_t^{-1} L_z w) \end{aligned}$$

$$\begin{aligned}
 & w(x, y, z, t) - w(x, y, z, 0) \\
 & \quad = D (L_t^{-1} L_{xx}w + L_t^{-1} L_{yy}w + L_t^{-1} L_{zz}w) \\
 & \quad \quad - A (L_t^{-1} L_xw + L_t^{-1} L_yw + L_t^{-1} L_zw) \\
 & w(x, y, z, t) = w(x, y, z, 0) + D L_t^{-1} (L_{xx}w + L_{yy}w + L_{zz}w) \\
 & \quad \quad - A (L_t^{-1} L_xw + L_t^{-1} L_yw + L_t^{-1} L_zw) \tag{17}
 \end{aligned}$$

In ADM, represent the solution suppose that

$$w(x, y, z, t) = \sum_{n=0}^{\infty} w_n(x, y, z, t) \tag{18}$$

Substituting Eq. (18) into (17), getting that

$$\begin{aligned}
 \sum_{n=0}^{\infty} w_n(x, y, z, t) &= w(x, y, z, 0) + D L_t^{-1} [L_{xx} \sum_{n=0}^{\infty} w_n(x, y, z, t) + \\
 & L_{yy} \sum_{n=0}^{\infty} w_n(x, y, z, t) + L_{zz} \sum_{n=0}^{\infty} w_n(x, y, z, t)] - A L_t^{-1} [L_x \sum_{n=0}^{\infty} w_n(x, y, z, t) + \\
 & L_y \sum_{n=0}^{\infty} w_n(x, y, z, t) + L_z \sum_{n=0}^{\infty} w_n(x, y, z, t)] \\
 w_0(x, y, z, t) + w_1(x, y, z, t) + \dots &= w(x, y, z, 0) + \\
 D L_t^{-1} [L_{xx} \sum_{n=0}^{\infty} w_n(x, y, z, t) + L_{yy} \sum_{n=0}^{\infty} w_n(x, y, z, t) + L_{zz} \sum_{n=0}^{\infty} w_n(x, y, z, t)] - & \tag{19} \\
 A L_t^{-1} [L_x \sum_{n=0}^{\infty} w_n(x, y, z, t) + L_y \sum_{n=0}^{\infty} w_n(x, y, z, t) + L_z \sum_{n=0}^{\infty} w_n(x, y, z, t)]
 \end{aligned}$$

Now, comparing the Eq. (19) on both sides getting the recurrent relation in the form of as follows

$$w_0(x, y, z, t) = w(x, y, z, t_0) = \phi_0(x, y, z) \text{ (From Eq. (2))}$$

and

$$\begin{aligned}
 w_{n+1}(x, y, z, t) &= D L_t^{-1} (L_{xx}w_n(x, y, z, t) + L_{yy}w_n(x, y, z, t) + L_{zz}w_n(x, y, z, t)) - \\
 & A L_t^{-1} (L_xw_n(x, y, z, t) + L_yw_n(x, y, z, t) + L_zw_n(x, y, z, t)) \quad \text{for } n = 0, 1, 2, \dots
 \end{aligned}$$

From which

$$\begin{aligned}
 w_1(x, y, z, t) &= D L_t^{-1} (L_{xx}w_0(x, y, z, t) + L_{yy}w_0(x, y, z, t) + L_{zz}w_0(x, y, z, t)) \\
 & \quad - A L_t^{-1} (L_xw_0(x, y, z, t) + L_yw_0(x, y, z, t) + L_zw_0(x, y, z, t)) \\
 w_2(x, y, z, t) &= D L_t^{-1} (L_{xx}w_1(x, y, z, t) + L_{yy}w_1(x, y, z, t) + L_{zz}w_1(x, y, z, t)) \\
 & \quad - A L_t^{-1} (L_xw_1(x, y, z, t) + L_yw_1(x, y, z, t) + L_zw_1(x, y, z, t)) \tag{20} \\
 & \quad \quad \quad \vdots \\
 w_n(x, y, z, t) &= D L_t^{-1} (L_{xx}w_{n-1}(x, y, z, t) + L_{yy}w_{n-1}(x, y, z, t) + L_{zz}w_{n-1}(x, y, z, t) \\
 & \quad - A L_t^{-1} (L_xw_{n-1}(x, y, z, t) + L_yw_{n-1}(x, y, z, t) + L_zw_{n-1}(x, y, z, t))
 \end{aligned}$$

Therefore, the estimation of the approximate solution  $\phi_\gamma$  by using  $\gamma$ -term approximation. That is,

$$\phi_\gamma = \sum_{n=0}^{\gamma-1} w_n(x, y, z, t) \quad (21)$$

Therefore, Eq. (21) is the approximate solution of the 3-D diffusion-advection mathematical model.

#### 2.4 Water Pollution Estimation

The DF mathematical approach estimates the water pollution level at a 3-D grid location over a time interval, whose result is validated by comparing it with the ADM approach. Eq. (15) estimates the pollutant concentration in water at different locations over time by the DF method. It is a 3-level explicit method, in which the current time ( $t + 1$ ) water pollution level at a particular location is estimated by using the surrounding locations' value in  $x, y$  and  $z$  directions of the previous one-time level ( $t$ ) and the respective location value of the last two-time level ( $t - 1$ ). This method simulates the spread of pollutants, such as an iodized salt-water solution, in a water body, helping us understand how contamination disperses.

Eq. (21) represents the pollutant concentration in water at any given point  $(x, y, z)$  and time  $t$ , using a series solution derived from the ADM. The formula states that the analytical solution is a sum of the terms  $w_0, w_1, w_2, \dots, w_{\gamma-1}$ . Here,  $w_0$  is an initial condition, and Eq. (20) is used to calculate the remaining terms,  $w_1, w_2, \dots, w_{\gamma-1}$ . Thus, this equation provides a way to calculate the concentration of pollutants over time and space using a series expansion approach.

### 3 Experimented Result and Discussion

The proposed work extends the diffusion-advection model into a 3-D region to estimate water pollution. Furthermore, we have demonstrated the 3-D water pollution model in a 3-D dummy cuboid water tank having dimensions  $4.25 \times 4.25 \times 2.25$  feet in *length*  $\times$  *breath*  $\times$  *height*. A 3-D grid structure has been placed in the 3-D cuboid tank, with a distance of one foot between each grid in all directions. Each 3-D grid location represents approximately one cubic feet of water volume area, so that the total volume of tank is covered within 75 grid locations. As a result, it is assumed that the amount of pollutant present at a particular location will be consider as the average pollution of one cubic foot water volume area. Thus, this grid setup helps to study the pollution spreads in all three directions inside the tank. Here, in experiments total 960 litres water is used in a tank as a medium of pollute, whereas 40-litres iodized salt-water solution is used as a pollutant, and the polluted water is measured in PPM by Total Dissolved Solids (TDS) meter over every 20 minutes of the time interval. The different types of 3-D grid locations based on their respective position in the cuboid water tank have been presented in Fig. 2.

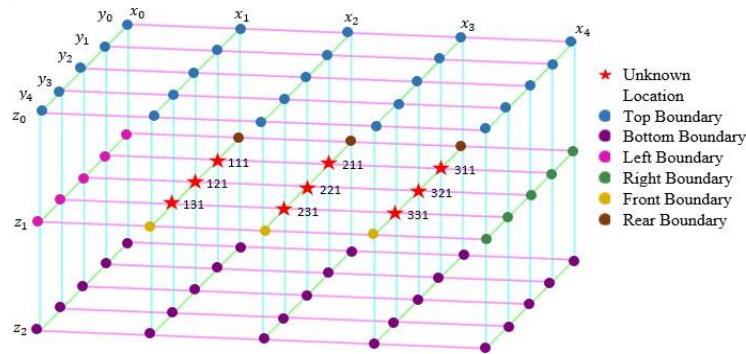


**Fig. 2** 3-D Grid Locations

Here, the 3-D grid locations in  $x, y$  and  $z$  space direction are set as  $r = 4, s = 4, p = 2$  and  $l = 8$  respectively in Eq. (4) so that the space intervals can be defined as;  $x_0 \leq x \leq x_4, y_0 \leq y \leq y_4, z_0 \leq z \leq z_2$  and the time interval would be  $t_0 \leq t \leq t_8$ . Furthermore, considering  $x_0 = y_0 = z_0 = t_0 = 0, x_4 = y_4 = 4, z_2 = 2$  and  $t_8 = 8$ , the range of different types of 3-D grid locations can be classified as in the Table 1.

**Table 1** Types of 3-D grid locations

Types	3-D grid locations
Left Boundary	$x = 0, 0 \leq y \leq 4, 0 < z < 2$
Right Boundary	$x = 4, 0 \leq y \leq 4, 0 < z < 2$
Rear Boundary	$0 < x < 4, y = 0, 0 < z < 2$
Front Boundary	$0 < x < 4, y = 4, 0 < z < 2$
Top Boundary	$0 \leq x \leq 4, 0 \leq y \leq 4, z = 0$
Bottom Boundary	$0 \leq x \leq 4, 0 \leq y \leq 4, z = 2$
Unknown	$(x_1 = 1) < x < (x_3 = 3),$ $(y_1 = 1) \leq y \leq (y_3 = 3),$ $z = (z_1 = 1)$

The mathematical model is implemented with spatial increments of 1 foot in the  $x, y,$  and  $z$  directions and a time step of 1 unit, which is equal to 20 minutes. Fig. 3 shows the visual representation of the Exp. data across different time intervals.

Time	$t = 0$	$t = 1$	$t = 2$
------	---------	---------	---------

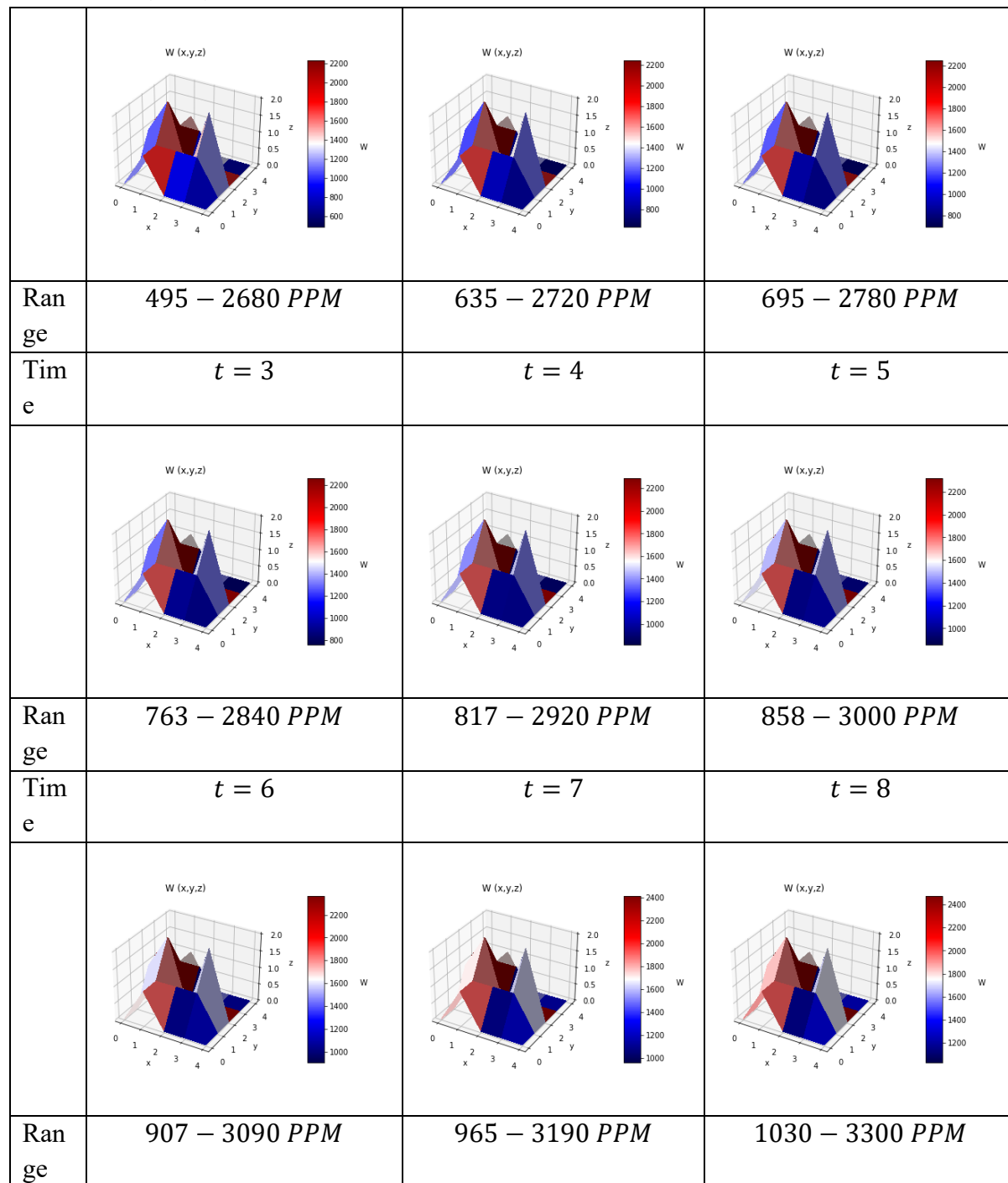


**Fig. 3** Water pollution at 3-D grid locations of Exp. data

Fig. 3 show that at the initial time  $t = 0$ , the level of water pollution is in range from minimum 495 PPM to the maximum 2680 PPM. After the 180 minutes, the minimum water pollution level is 1030 PPM and maximum pollution level is 3300 PPM. Therefore, the level of water pollution is going to be increased with every 20 minutes of time interval at each 3-D grid location.

The required initial and boundary conditions for time and space are derived using a Multi-Poly Regression model on the obtained Exp. data, which can be expressed as in Eq. (22) – (29) with

their respective Mean Absolute Error (MAE) and Standard Deviation of Mean Absolute Error ( $SD_{MAE}$ ).

Initial and Boundary Conditions	MAE	$SD_{MAE}$	
Initial Condition for time $t = (t_0 = 0)$			
$w(x, y, z, 0) = 903.55 * z - 71.87 * z^2 - 73.67 * y - 78.60 * y * z + 24.22 * y * z^2 + 6.24 * y^2 + 5.34 * y^2 * z - 2.86 * y^2 * z^2 - 325.08 * x - 117.94 * x * z + 49.86 * x * z^2 + 44.60 * x * y + 5.69 * x * y * z - 3.57 * x * y * z^2 - 3.98 * x * y^2 + 0.45 * x * y^2 * z + 213.34 * x^2 - 21.77 * x^2 * z + 2.06 * x^2 * z^2 - 19.12 * x^2 * y + 1.87 * x^2 * y * z + 0.23 * x^2 * y^2 - 73.13 * x^3 + 0.05 * x^3 * z + 2.69 * x^3 * y + 1159.17 + 8.26 * x^4;$	0.0014	0.0011	(22)
Initial Condition for time $t = (t_1 = 1)$			
$w(x, y, z, 1) = 892.39 * z - 70.96 * z^2 - 70.69 * y - 78.28 * y * z + 25.18 * y * z^2 + 4.60 * y^2 + 6.03 * y^2 * z - 3.31 * y^2 * z^2 - 407.39 * x - 111.71 * x * z + 51.25 * x * z^2 + 46.17 * x * y + 4.81 * x * y * z - 3.44 * x * y * z^2 - 3.35 * x * y^2 + 0.49 * x * y^2 * z + 244.99 * x^2 - 24.97 * x^2 * z + 1.54 * x^2 * z^2 - 19.65 * x^2 * y + 1.94 * x^2 * y * z + 0.11 * x^2 * y^2 - 76.46 * x^3 + 0.58 * x^3 * z + 2.83 * x^3 * y + 1219.93 + 8.63 * x^4;$	0.0012	0.0009	(23)
Left Boundary			
$w(0, y, z, t) = 50.15 * t + 1989.34 * z + 4.43 * z * t^2 + 2.22 * y * t + 0.04 * y * t^2 - 128.40 * y * z + 9.22 * y^2 - 1.04 * y^2 * t - 0.093 * y^3;$	0.0012	0.00076	(24)
Right Boundary			
$w(4, y, z, t) = -0.12 * y * t^2 - 1.22 * y^2 * t + 958 + 106.32 * t + 4.04 * t^2 - 47.04 * y + 11.88 * y * t - 1.44 * y^2 - 1.47e - 14 * y^3;$	0.0011	0.00085	(25)
Rear Boundary			
$w(x, 0, z, t) = 42.23 * t + 1812.02 * z + 5.076 * z * t^2 - 69.87 * x * t - 0.43 * x * t^2 - 91.36 * x^2 + 21.83 * x^2 * t + 9.56 * x^3;$	0.0012	0.0008	(26)
Front Boundary	0.0019	0.0012	(27)

$$w(x, 4, z, t) = 40.08 * t + 4.8 * t^2 + 1504.56 * z - 0.27 * x * t^2 - 65.76 * x * t + 22.35 * x^2 * t - 76.76 * x^2 + 5.88 * x^3;$$

Top Boundary

$$w(x, y, 0, t) = 55.20 * t + 4.54 * t^2 - 72.73 * y + 1.76 * y * t + 0.048 * y * t^2 + 5.86 * y^2 - 0.99 * y^2 * t - 0.007 * y^2 * t^2 - 325.096 * x - 74.92 * x * t - 0.17 * x * t^2 + 42.35 * x * y + 2.14 * x * y * t - 0.0007 * x * y * t^2 - 3.51 * x * y^2 - 0.046 * x * y^2 * t + 214.80 * x^2 + 22.88 * x^2 * t - 0.011 * x^2 * t^2 - 18.21 * x^2 * y - 0.022 * x^2 * y * t + 0.13 * x^2 * y^2 - 74.013 * x^3 - 0.087 * x^3 * t + 2.59 * x^3 * y + 1159.17 + 8.39 * x^4; \quad 0.0015 \quad 0.0012 \quad (28)$$

Bottom Boundary

$$w(x, y, 2, t) = 2675.5 + 42.94 * t + 4.38 * t^2 - 130.74 * y + 3.02 * y * t + 0.002 * y * t^2 + 0.025 * y^2 * t^2 + 4.8 * y^2 - 1.18 * y^2 * t - 353.56 * x - 75.64 * x * t - 0.34 * x * t^2 - 0.023 * x * y * t^2 + 39.9 * x * y + 2.38 * x * y * t - 0.043 * x * y^2 * t - 2.58 * x * y^2 + 0.059 * x^2 * t^2 + 176.82 * x^2 + 23.54 * x^2 * t - 0.029 * x^2 * y * t - 15.7 * x^2 * y + 0.17 * x^2 * y^2 - 0.27 * x^3 * t - 73.82 * x^3 + 2.82 * x^3 * y + 8.43 * x^4; \quad 0.0012 \quad 0.0009 \quad (29)$$

In the experiment of a proposed mathematical model, it is necessary to fix the value of the diffusion rate and advection rate of the iodized salt-water solution into the volume of the water tank. The diffusion rate is derived based on the phenomena of Fick's first law, which is defined in Eq. (30) [23].

$$D = -D_v \frac{dC}{df} \quad (30)$$

Where,  $D$  is the diffusion rate,  $D_v$  is the diffusivity value of iodized salt-water solution ( $\text{cm}^2/\text{s}$ ), and  $\frac{dC}{df}$  is the average concentration gradient. In Eq. (30), the negative sign denotes that the flow proceeds from the area of high concentration to the area of low concentration.

The diffusivity value of iodized salt-water solution can be derived from Eq. (31).

$$D_v = \frac{4 V x_c}{\pi d^2 N M C_M} \frac{dk}{dt} \quad (31)$$

Here,  $V$  is the volume of water in diffusion vessel (Liter (L) or  $\text{cm}^3$ ),  $x_c$  is the capillaries' length (cm),  $d$  is the diameter of capillaries (cm),  $N$  is the number of capillaries,  $M$  is the molar concentration of iodized salt water solution (mol/L),  $C_M$  is the slope of conductivity change per

unit molar concentration change ( $\mu\text{S}\cdot\text{L}/\text{mol}$ ) and  $\frac{dk}{dt}$  is the slope of conductivity change per unit time ( $\mu\text{S}/\text{s}$ ).

In this experiment,  $V = 2500 \text{ cm}^3$ ,  $x_c = 0.4 \text{ cm}$ ,  $d = 0.1 \text{ cm}$ ,  $N = 50$ . The molar concentration of iodized salt is

$$M = \frac{w_s}{M_w} \times \frac{1 \text{ (L)}}{V_s} \quad (32)$$

Where,  $w_s$  is the weight of solute (gm),  $M_w$  is the molecular weight of solute (gm/mol) and  $V_s$  is the volume of solvent (L).

Here,  $w_s = 2500 \text{ gm}$  iodized salt

$$\begin{aligned} M_w &= Na^+ + Cl^- + I^- + Mg^+ (\text{impurity}) \\ &= 23 + 35.5 + 127 + 24 = 209.5 \text{ gm/mol} \end{aligned}$$

$$V_s = 40 \text{ L}$$

Substituting these values into Eq. (32), that

$$M = \frac{2500 \text{ gm}}{209.5 \text{ gm/mol}} \times \frac{1 \text{ L}}{40 \text{ L}}$$

$$M = 0.29 \text{ mol/L}$$

The experiment shows that the conductivity of iodized salt water solution is changed as its molar concentration level is vary. Based on the results obtained during experiment the slope of conductivity per unit molar concentration ( $C_M$ ) is measured from curve fitting of conductivity Vs. molar concentration which is graphically presented in Fig. 4. Furthermore, in the experiment it is observed that the conductivity is varying as the time changed. Based on the experimented results the conductivity changes per unit time ( $\frac{dk}{dt}$ ) is obtained by curve fitting between conductivity Vs. time as graphically presented in Fig. 5.

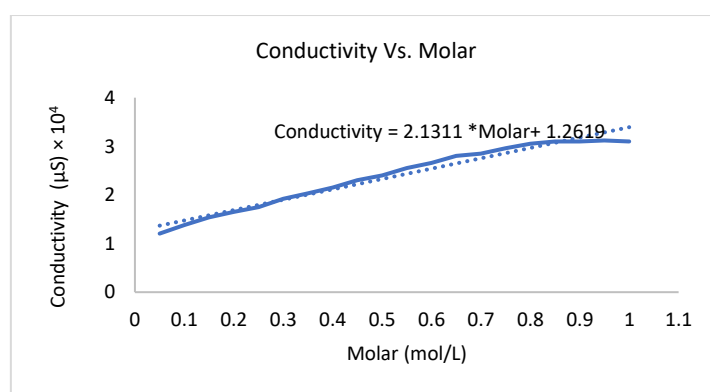


**Fig. 4** Conductivity Vs. Molar

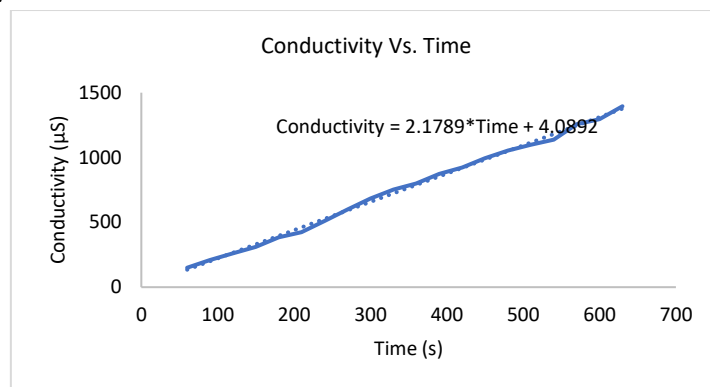


**Fig. 5** Conductivity Vs. Time

Fig. 4 and 5 shows that, the coefficient of molar indicates slope of the conductivity change per unit molar concentration  $C_M = 2.1311 \times 10^4 \frac{\mu S \cdot L}{mol}$  and the coefficient of time indicated the slope of conductivity change per unit time  $\frac{dk}{dt} = 2.1789 \mu S/s$ . Now, substituting all the required values in Eq. (31), getting that

$$D_v = \frac{4 \times 2500 \text{ cm}^3 \times 0.4 \text{ cm} \times 2.1789 \mu S/s}{3.14 \times (0.1)^2 \text{ cm}^2 \times 50 \times 0.29(\text{mol/L}) \times 2.1311 \times 10^4 (\mu S \cdot L)/\text{mol}}$$

$$D_v = \frac{8715.6}{0.97028 \times 10^4} \frac{\text{cm}^2}{s}$$

$$D_v = 8982.56 \times 10^{-4} \frac{\text{cm}^2}{s}$$

In the experiment, the  $z$  – axis has three different layers as  $0 \leq z \leq 2$  such as 1<sup>st</sup> layer (Top), 2<sup>nd</sup> layer (Middle) and 3<sup>rd</sup> layer (Bottom) of cuboid tank.

Now, the average value of the concentration gradient for 1<sup>st</sup> and 2<sup>nd</sup> layer is

$$\left(\frac{dC}{df}\right)_1 = \frac{c_2 - c_1}{f_2 - f_1} \tag{33}$$

and for 2<sup>nd</sup> and 3<sup>rd</sup> layer is

$$\left(\frac{dC}{df}\right)_2 = \frac{c_3 - c_2}{f_3 - f_2} \tag{34}$$

where,  $c_1$  is the average of 1<sup>st</sup> layer ( $z = 0$ ) pollution =  $1387.219 \frac{PPM}{\text{cm}^3}$ ,  $c_2$  is the average of 2<sup>nd</sup> layer ( $z = 1$ ) pollution =  $1381.575 \frac{PPM}{\text{cm}^3}$ ,  $c_3$  is the average of 3<sup>rd</sup> layer ( $z = 2$ ) pollution =  $1372.26 \frac{PPM}{\text{cm}^3}$ . Moreover,  $f_1, f_2, f_3$  are the distance (cm) between layers. Here,  $f_1 = 0$  feet = 0 cm,  $f_2 = 1$  feet = 30.48 cm,  $f_3 = 2$  feet = 60.96 cm. Now, substituting all these values in Eq. (33) and (34), getting that  $\left(\frac{dC}{df}\right)_1 = -0.185 \frac{PPM}{\text{cm}^4}$  and  $\left(\frac{dC}{df}\right)_2 = -0.3056 \frac{PPM}{\text{cm}^4}$  whose average value is of  $\frac{dC}{df} = -0.24 \frac{PPM}{\text{cm}^4}$ . By applying all the required values in Eq. (30), gets Eq. (35)

$$\begin{aligned}
 D &= -8982.56 \times 10^{-4} \frac{\text{cm}^2}{\text{s}} \times -0.24 \frac{\text{PPM}}{\text{cm}^4} \\
 D &= 2155.8 \times 10^{-4} \frac{\text{PPM}}{\text{cm}^2 \text{ s}} \\
 D &= 0.21558 \frac{\text{PPM}}{\text{cm}^2 \text{ s}}
 \end{aligned} \tag{35}$$

The diffusion rate has been calculated using the principles of Fick's First Law, which produced a value of  $D = 0.21558 \text{ PPM}/(\text{cm}^2 \text{ s})$ . To fix the value of advection rate, the principle of advective flux, as defined in Eq. (36), has been used.

$$A = v \times c_s \tag{36}$$

Where,  $A$  is the advection rate,  $v$  is the in-flow velocity of pollutant and  $c_s$  is the concentration of solute i.e. dissolution of amount of pollutant in per unit volume of pollute.

Here, in the experiment the in-flow velocity of pollutant is measured as

$$\begin{aligned}
 v &= \frac{1}{5} \text{ ft/sec} \\
 &= \frac{30.48}{5} \text{ cm/sec} \\
 v &= 6.096 \text{ cm/sec}
 \end{aligned} \tag{37}$$

And the concentration of solute, is

$$\begin{aligned}
 c_s &= \frac{20}{1} \text{ ml}/(\text{ft}^3) \\
 &= \frac{20}{28.3168} \text{ ml}/\text{ltr} \\
 &= \frac{20}{28316.8} \text{ ml}/\text{ml} \\
 c_s &= 0.00070629
 \end{aligned} \tag{38}$$

Substituting the value of Eq. (37) and (38) in (36), that the advection rate is

$$\begin{aligned}
 A &= 6.096 \text{ cm/sec} \times 0.00070629 \\
 A &= 0.004305 \text{ cm/sec}
 \end{aligned} \tag{39}$$

The proposed mathematical model is simulated by considering  $\delta x = \delta y = \delta z = 1$  feet, and  $\delta t = 1$  unit (20 minutes), and the diffusion rate  $D = 0.21558 \frac{\text{PPM}}{\text{cm}^2 \text{ s}}$  and advection rate  $A = 0.004305 \text{ cm/sec}$  is considered similar in all the directions  $x, y$  and  $z$ .

At different 3-D grid locations, the DF solution is obtained by applying the corresponding  $x, y, z$  and  $t$  value to Eq. (15) with the initial and boundary conditions given in Eq. (22) - (29). The numerical solution of Eq. (1), which computed using the DF method is displayed in Fig. 6.

Time	$t = 0$	$t = 1$	$t = 2$
Range	495.52 – 2678.80 PPM	635.10 – 2720.87 PPM	696.07 – 2778.91 PPM
Time	$t = 3$	$t = 4$	$t = 5$
Range	763.89 – 2843.78 PPM	817.91 – 2917.41 PPM	858.61 – 2999.82 PPM

Time	$t = 6$	$t = 7$	$t = 8$
Range	907.80 – 3091.005 PPM	965.45 – 3190.96 PPM	1031.59 – 3299.69 PPM

**Fig. 6** Water pollution at 3-D grid locations by DF

The water pollution concentration at the initial time  $t = 0$  varied from a minimum of 495.52 PPM to a maximum of 2678.80 PPM, as shown in Fig. 6. The values increased to a minimum of 1031.59 PPM and a maximum of 3299.69 PPM after 180 minutes. Fig. 6 clearly indicates

that the water pollution levels are rising with time in all 3-D grid locations. A significant increment in water pollution to be noted can also be increased as the time passed up to its saturation limit.

Although the DF method has given a numerical solution of the given 3-D diffusion model for water pollution that reflects the real-time phenomena that actually happened during the experiment, another mathematical solution approach should be adopted to validate the obtained results. Thus, the proposed diffusion-advection model will be solved analytically using the ADM to predict water pollution levels at the same 3-D grid locations throughout the same time period for ensuring the accuracy of the numerical results. The required analytic function of Eq. (1) is derived by using the Eq. (21). It is determined by adding the term of  $w_0, w_1, w_2, \dots, w_{\gamma-1}$ .  $w_0$  is the initial conditions and remaining terms are determined by using the Eq. (20).

In this study, only the terms  $w_0, w_1, w_2, w_3$  and  $w_4$  are used to create the analytical function of Eq. (1) due to the initial condition's polynomial nature (degree 4). The higher-order terms above  $w_4$  are disappear because after the  $w_4$  term the first order derivative does not exist. Therefore, the terms from  $n = 0$  to 4 are included in the analytical function. The analytic function of Eq. (1) are as follows:

$$\begin{aligned}
 w(x, y, z, t) = & 9.199 * A^4 * t^4 + t^3 * (-46.49 * A^3 * x + 3.353 * A^3 * y + \\
 & 6.344 * A^3 * z + 32.9 * A^3 + 110.9 * A^2 * D) + t^2 * (61.97 * A^2 * x^2 + 10.07 * \\
 & A^2 * x * y + 5.466 * A^2 * x * z - 249.6 * A^2 * x - 2.174 * A^2 * y^2 - 15.78 * A^2 * \\
 & y * z + 13.5 * A^2 * y - 4.358 * A^2 * z^2 + 137.4 * A^2 * z - 4.228 * A^2 - 217.7 * \\
 & A * D * x - 2.246 * A * D * y - 1.771 * A * D * z + 369.7 * A * D + 96.91 * \\
 & D^2) + t * (-A * (35.8 * x^3 + 10.4 * x^2 * y + 6.146 * x^2 * z - 260.3 * x^2 + \\
 & 0.9128 * x * y^2 - 2.487 * x * y * z - 40.52 * x * y + 0.5636 * x * z^2 + 61.87 * \\
 & x * z + 353.3 * x - 5.261 * y^2 * z + 1.357 * y^2 - 9.279 * y * z^2 + 64.8 * y * z - \\
 & 21.52 * y + 74.08 * z^2 - 340.3 * z + 504.8) + D * (103.8 * x^2 + 9.02 * x * y + \\
 & 1.207 * x * z - 347 * x - 5.255 * y^2 + 3.736 * y * z + 10.19 * y - 1.586 * z^2 - \\
 & 32.87 * z + 295.4)) + 8.264 * x^4 + 2.692 * x^3 * y + 0.05 * x^3 * z - 73.13 * x^3 + \\
 & 0.2296 * x^2 * y^2 + 1.868 * x^2 * y * z - 19.12 * x^2 * y + 2.064 * x^2 * z^2 - \\
 & 21.77 * x^2 * z + 213.3 * x^2 + 0.4536 * x * y^2 * z - 3.979 * x * y^2 - 3.565 * x * \\
 & y * z^2 + 5.689 * x * y * z + 44.6 * x * y + 49.86 * x * z^2 - 117.9 * x * z - \\
 & 325.1 * x - 2.857 * y^2 * z^2 + 5.336 * y^2 * z + 6.238 * y^2 + 24.22 * y * z^2 - \\
 & 78.6 * y * z - 73.67 * y - 71.87 * z^2 + 903.5 * z + 1159
 \end{aligned} \tag{40}$$

Now, solving Eq. (40) by substituting the value of the diffusion rate  $D$  and advection rate  $A$  derived in Eq. (35) and (39) respectively and  $x, y, z$  and  $t$  alternating that gives the level of water pollution at all 3-D grid locations. Fig. 7 displays a graphical representation of the ADM's outcomes for the water pollution level at each 3-D grid location over the time period.

Time	$t = 0$	$t = 1$	$t = 2$

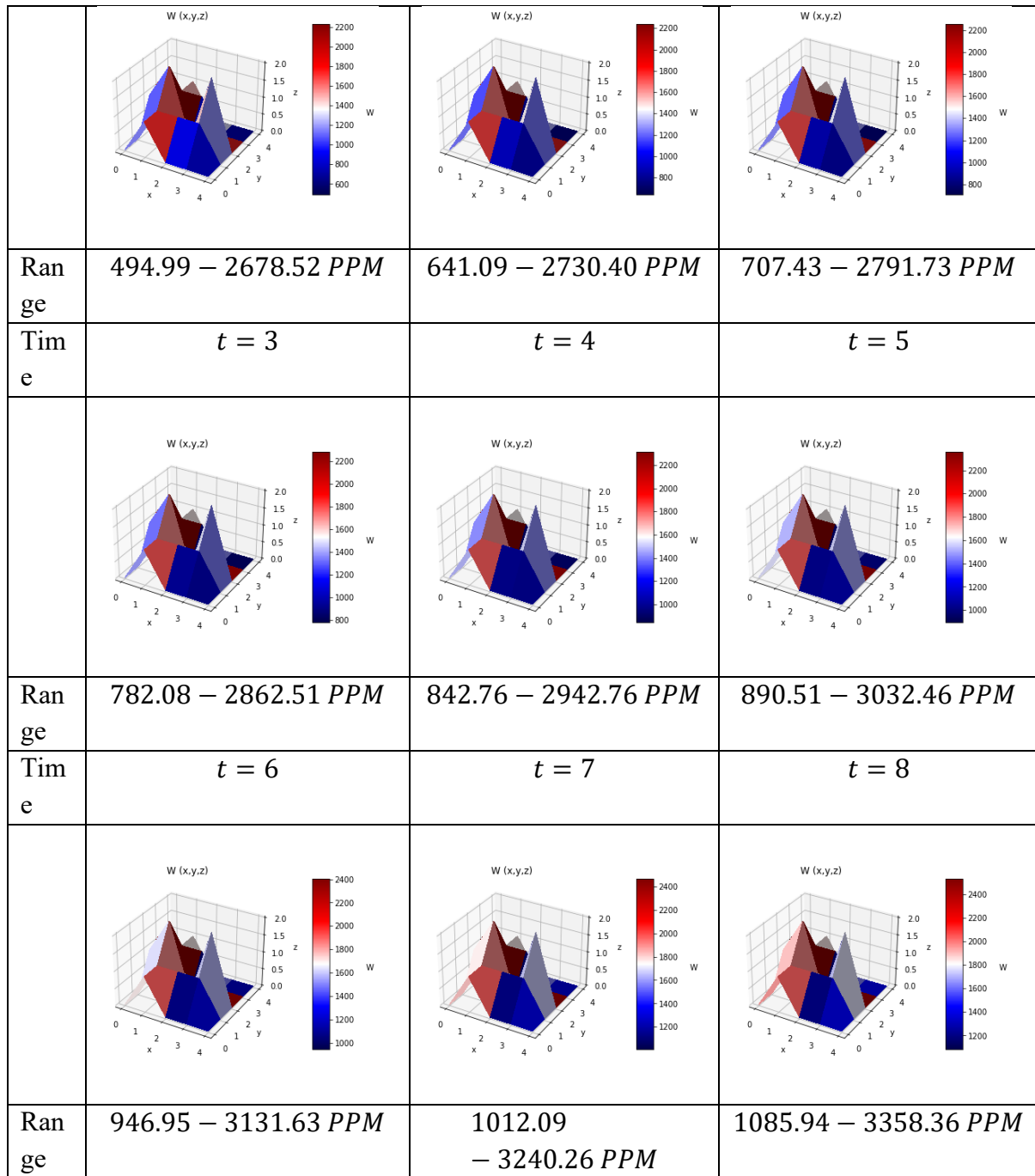


**Fig. 7** Water pollution at 3-D grid locations by ADM

Fig. 7 shows that, at several locations around the 3-D grid, it is visible that the level of water pollution steadily rises over time. At  $t = 0$  time level the water pollution minimum level is 494.99 PPM and maximum level is 2678.52 PPM. After time passes, at  $t = 8$ , the level of water pollution is 1085.94 – 3358.36 PPM. There has been a monotonically increment in water pollution at different locations with respect to the time interval.

Two different approaches have been used to solve Eq. (1): ADM and DF which gives the analytic and numerical results respectively. The outputs of the numerical approaches are compared with Exp. data and the analytical results from ADM in order to assess the accuracy of these solutions. The error estimation criteria are used for the comparison, which can be

obtained by taking the absolute difference between the water pollution levels at each 3-D grid location across the time interval. The estimated error is graphically plotted in Fig. 8.

<i>Time</i>	<i>DF vs Exp. Data</i>	<i>DF vs ADM</i>
<i>t = 0</i>		
<i>Range</i>	<b>0.015 – 6.66 PPM</b>	<b>0.15 – 0.94 PPM</b>
<i>t = 1</i>		
<i>Range</i>	<b>0.011 – 5.46 PPM</b>	<b>0.054 – 10.07 PPM</b>
<i>t = 2</i>		
<i>Range</i>	<b>0.11 – 10.23 PPM</b>	<b>5.37 – 15.59 PPM</b>
<i>t = 3</i>		
<i>Range</i>	<b>0.029 – 13.86 PPM</b>	<b>9.73 – 22.63 PPM</b>
<i>t = 4</i>		

<i>Range</i>	<b>0.012 – 15.13 PPM</b>	<b>15.40 – 29.51 PPM</b>
<i>t = 5</i>		
<i>Range</i>	<b>0.18 – 13.62 PPM</b>	<b>22.09 – 36.25 PPM</b>
<i>t = 6</i>		
<i>Range</i>	<b>0.21 – 17.37 PPM</b>	<b>29.38 – 42.84 PPM</b>
<i>t = 7</i>		
<i>Range</i>	<b>0.032 – 16.93 PPM</b>	<b>37.05 – 51.31 PPM</b>
<i>t = 8</i>		
<i>Range</i>	<b>0.04 – 17.39 PPM</b>	<b>45.15 – 61.92 PPM</b>

**Fig. 8** Comparative analysis between DF Vs. Exp. data and ADM Results

Fig. 8 shows that, the comparative analysis between DF Vs. Exp. data has the error range in between 0.011 PPM to 17.39 PPM and 0.054 to 61.92 PPM in DF Vs. ADM. Also, the analysis of the comparative study between all 75 locations  $\times$  9 time intervals during the whole duration, it has been observed that the DF methods error against the Exp. data and ADM method is visually shown in Fig. 9 for both PPM difference (error)  $\leq 60$  and  $> 60$ .

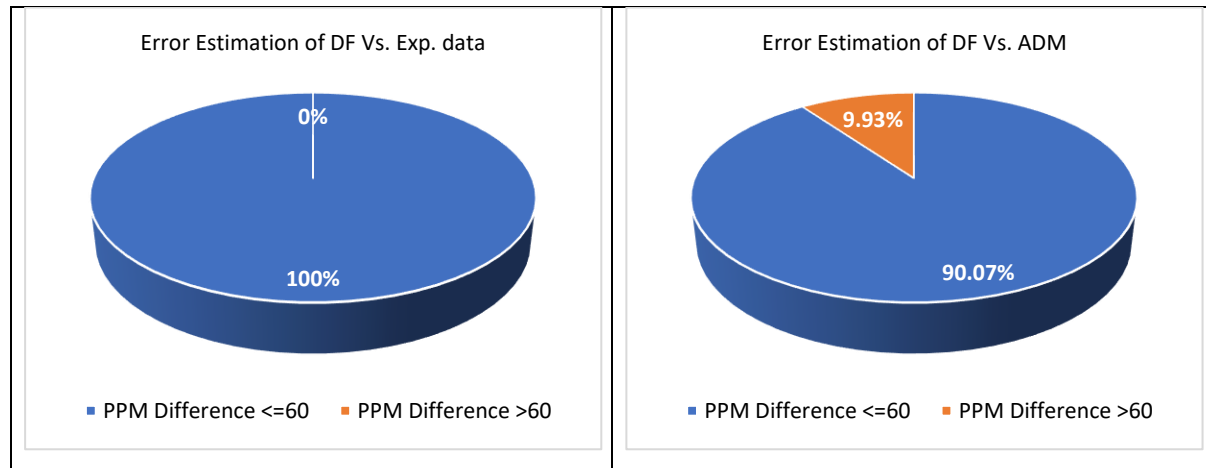


**Fig. 9** Error Estimation of DF Vs. Exp. data and ADM

Fig. 9 shows that, in DF Vs. Exp. data comparison, 100% of the PPM difference lies under 60 PPM which is highly negligible in the form of PPM because a change of up to 60 PPM is considered a negligible change while above 60 PPM represents a significant change in the level of water pollution [25,26]. As a result, it can be said that 100% of the PPM difference does not affect the water pollution level.

In DF vs. ADM comparisons, 90.07% of the observations have PPM difference below 60 PPM which is insignificant in the form of PPM, while only 9.93% exceed 60 PPM which does have significant impact on the change of water pollution level. Thus, DF methods results are validated with the Exp. data, the analytical solution obtained by the ADM method and implemented boundary conditions. It concludes that the result obtained by the DF method can be more reliable with the Exp. data than the analytical ADM results for predicting water pollution levels over a time interval.

As described in Table 1, there are several types of 3-D grid locations in cuboid water tank. In which, at every time interval, the water pollution level at the top, bottom, left, right, rear and front boundary locations is estimated based on the boundary conditions given in Eq. (24) – (29) while the water pollution level at nine unknown locations is calculated by DF method. These nine locations can be labelled as  $L_{xyz} : L_{111}, L_{121}, L_{131}, L_{211}, L_{221}, L_{231}, L_{311}, L_{321}, L_{331}$ . Here, it is essential to compare the water pollution level numerically obtained by DF with the Exp. data and the analytical values derived by the ADM approach at each time interval, graphically represented in Fig. 10.

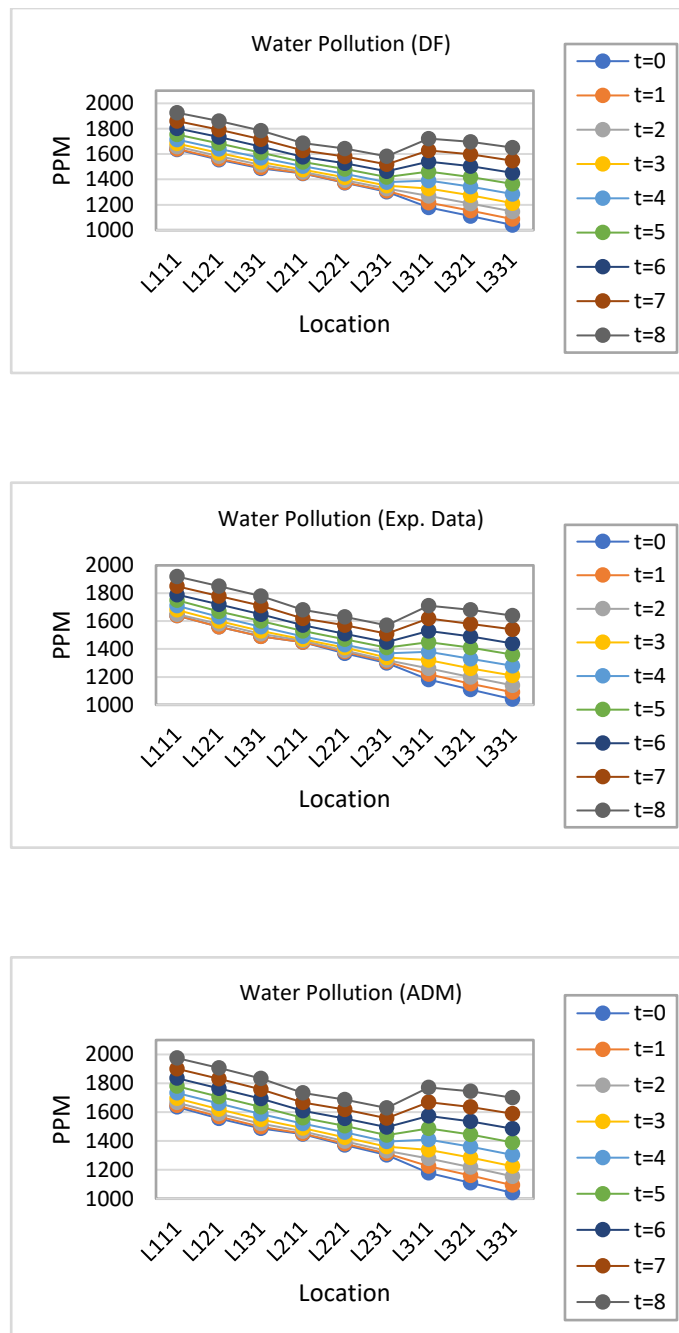


**Fig. 10** DF, Exp. data and ADM Result at Nine Unknown Locations

As shown in Fig. 10, the water pollution level at nine unknown locations gradually rise over time in all three cases: DF, Exp. data and ADM approach. This indicates that pollution of water is monotonically increasing over time in these locations. The DF approaches yield outcomes that more closely match the Exp. data at every time step and location than ADM results. The values provided by ADM vary from Exp. data than the corresponding values provided by DF method which is clear by observing the error between ADM and the DF approach.

Now, the variations in water pollution levels over time at particular unknown locations, as determined by the DF, ADM methods and the Exp. data, are shown in Fig. 11.

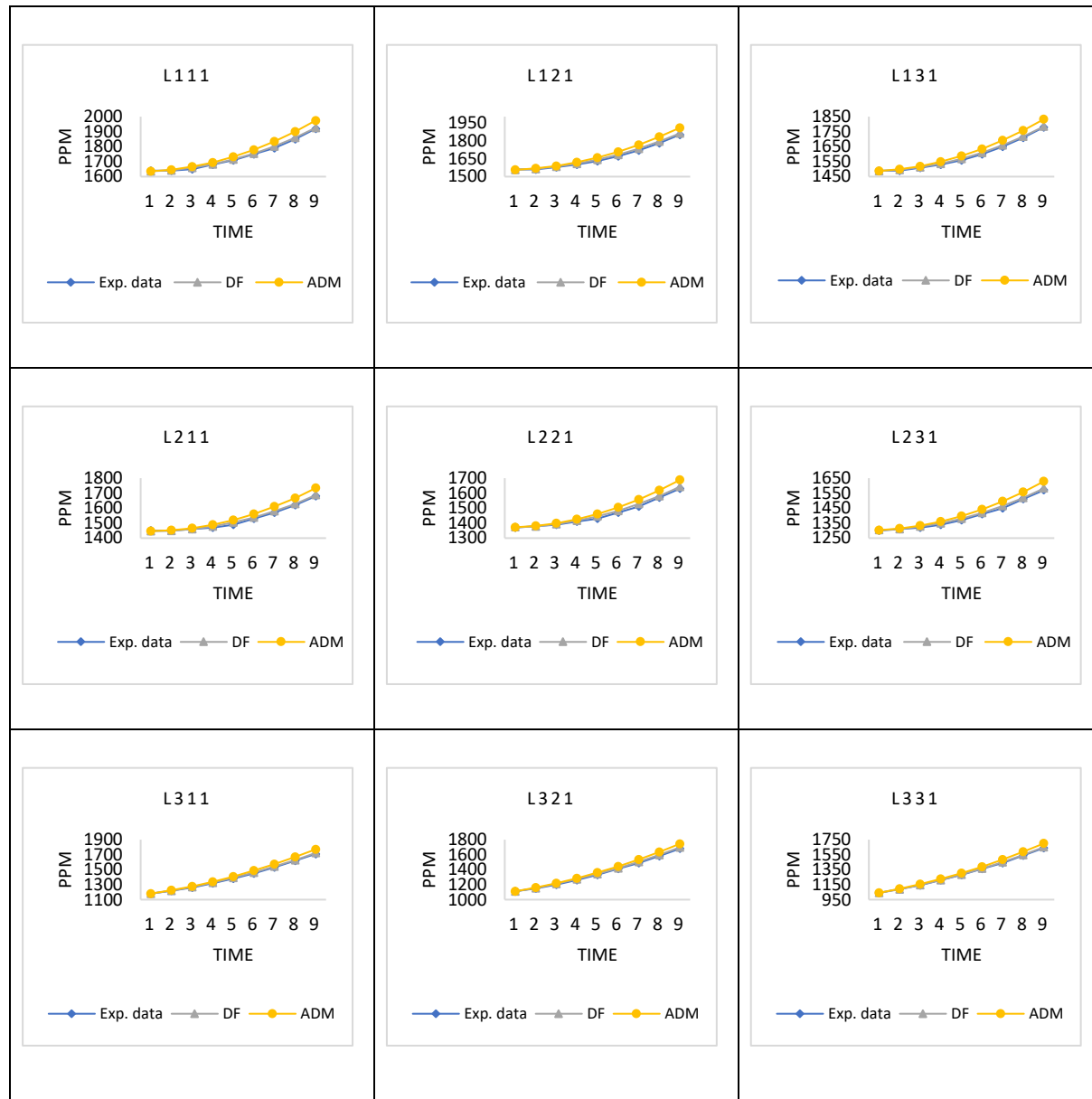


**Fig. 11** Water pollution level at unknown Location

Fig.11 shows that the graphs generated by each method are almost the same at every unknown place across time. This suggests that the various approaches to forecasting changes in water pollution levels over time provide seems identical outcomes. The error between the methods is insignificant because the graphs nearly overlap.

Therefore, the significant level of consistency between the outcomes indicates that the numerical DF method is trustworthy and useful for assessing water pollution in various kinds of scenarios.

#### 4 Conclusion

The current study effectively demonstrates a mathematical model utilizing a 3-D diffusion-advection framework to predict water pollution levels in a cuboid water tank. This research enhances the analysis by extending it into three spatial dimensions, enabling a more precise estimation of pollutant dispersion. Iodized salt water solution serves as the pollutant in the

experiment, yielding precise Exp. data for validation. Pollutant levels rise slowly over time, as indicated by both numerical outcomes from the DF method and analytical results from the ADM. In the DF approach, the increase in water pollution during the specified time period was at a minimum range of 536.07 PPM and at a maximum of 620.89 PPM, while in the ADM approach, the increase ranged from a minimum of 590.95 PPM to a maximum of 679.84 PPM across the cuboid water tank. Comparative analysis indicates that the differences in DF, ADM, and Exp. data are nearly the same. Additionally, the error analysis indicated that the fluctuations in pollution levels in DF with Exp. data are below 60 PPM, which is deemed an insignificant change in water pollution levels expressed in PPM when comparing DF with ADM, there have been significant change in the level of water pollution. This verifies that the DF method is a reliable numerical approach that corresponds with both analytical results and Exp. data. A reliable framework for forecasting water pollution in 3-D areas is provided by the verified 3-D diffusion-advection model. The reliability is validated by the strong agreement of methods, and the strategy can be extended to bigger natural water systems for oversight, pollution control, and water quality management.

### **Declaration of Competing Interests**

The authors declare that they have no known competing financial interests or personal relationships that could have appeared to influence the work reported in this paper.

### **Research Funding**

This research received no specific grant from any funding agency in the public, commercial, or not-for-profit sectors.

### **Authors contribution**

**Tarjani Naik:** Conceptualization, Methodology / Study design, Validation, Formal analysis, Resources, Investigation, Data curation, Writing – original draft, Writing – review and editing, Visualization. **Mukesh Patel:** Conceptualization, Conceptualization, Validation, Formal analysis, Writing – original draft, Supervision. **Rachna Patel:** Software, Formal analysis, Resources, Data curation.

### **Data Availability**

The data that support the findings of this study are available on request from the corresponding author, [*Mukesh Petel, mukesh.mt@gmail.com*]. The data are not publicly available due to [restrictions e.g. their containing information that could compromise the privacy of research participants]

### **References**

- [1] Hanani Johari, Nursalasawati Rusli, and Zainab Yahya: Finite Difference Formulation for Prediction of Water Pollution. Materials Science and Engineering. (2018), doi: 10.1088/1757-899X/318/1/012005.
- [2] J. Bartram & R. Balance: Water quality monitoring: a practical guide to the design and implementation of freshwater quality studies and monitoring programmes. ResearchGate. (1996).

- [3] Busayamas Pimpunchata, Winston L. Sweatman, Graeme C. Wake, Wannapong Triampo, Aroon Parshotam: A mathematical model for pollution in a river and its remediation by aeration. *Applied Mathematics Letters*. **22**(3), 304-308 (2009), doi: 10.1016/j.aml.2008.03.026.
- [4] G. Tchobanoglous, F.L. Burton: *Wastewater Engineering: Treatment, Disposal and Reuse*. Environment Science, Engineering, 3 ed., McGraw-Hill, New York. (2002).
- [5] J. R. Zabadal, C. A. Poffal, S. B. Leite: Closed form solutions for water pollution problems-2. *Latin American Journal of Solids and Structures*. **3**(4), 377-392 (2006).
- [6] J. B. Shukla, A. K. Misra, Peeyush Chandra: Mathematical modeling and analysis of the depletion of dissolved oxygen in eutrophied water bodies affected by organic pollutants. *Nonlinear Analysis Real World Applications*. **9**(5), 1851-1865 (2008).
- [7] Nigar Sultana and Laek Sazzad Andallah: Investigation of Water Pollution in the River with Second-Order Explicit Finite Difference Scheme of Advection-Diffusion Equation and First-Order Explicit Finite Difference Scheme of Advection-Diffusion Equation. *Mathematical Statistician and Engineering Applications*. **71**(2), 12-27 (2022), doi: 10.17762/msea.v71i2.62.
- [8] Delong Wan, Huiping Zeng: Water environment mathematical model mathematical algorithm. *2<sup>nd</sup> International Symposium on Resource Exploration and Environmental Science*. **170**, (2018), doi: 10.1088/1755-1315/170/3/032133.
- [9] Nopparat Pochai, Suwon Tangmanee, L. J. Crane, J. J. H. Miller: A Mathematical Model of Water Pollution Control Using the Finite Element Method. *Proceedings in Applied Mathematics and Mechanics*. **6**(1), 755-756 (2006), doi: 10.1002/pamm.200610358.
- [10] Tsegaye Simon, Purnachandra Rao Koya: Modeling and Numerical Simulation of River Pollution using Diffusion-Reaction Equation. *American Journal of Applied Mathematics*. **3**(6), 335-340 (2015), doi: 10.11648/j.ajam.20150306.24.
- [11] R. V. Waghmare and S. B. Kiwne: Mathematical Modeling of Disposal of Pollutant in Rivers. *International Journal of Computational and Applied Mathematics*. **12**(3), 835-842 (2017).
- [12] Abbas Parsaie, Amir Hamzeh Haghiabi: Computational Modeling of Pollution Transmission in Rivers. *Applied Water Science*. **7**, 1213–1222 (2017), doi: 10.1007/s13201-015-0319-6.
- [13] Safia Meddah, Abdelkader Saidane, Mohamed Hadjel, Omar Hireche: Pollutant Dispersion Modeling in Natural Streams Using the Transmission Line Matrix Method. *Water*. **7**(9), 4932-4950 (2015), doi: 10.3390/w7094932.
- [14] A. Saravanan, N. Magesh: A comparison between the reduced Differential Transform Method and the Adomian Decomposition Method for the Newell-Whitehead-Segel equation. *Journal of the Egyptian Mathematical Society*. **21**(3), 259-265 (2013).
- [15] Snehashish Chakraverty, Nisha Mahato, Perumandla Karunakar, Tharasi Dilleswar Rao: Advanced numerical and semi analytical methods for differential equations. Wiley Telecom. 119-130 (2019), doi: 10.1002/9781119423461.ch11.
- [16] Ahmad M. D. Al-Eybani: Adomian Decomposition Method and Differential Transform Method to solve the Heat Equations with a power nonlinearity. *Ahmad M. D. Al-Eybani International Journal of Engineering Research and Application*. **5**(2), 94-98 (2015).

- [17] Srimanta Pal: Numerical Methods: Principles, Analysis and Algorithms. Oxford University Press. (2009).
- [18] A. Salih: Finite Difference Method for Parabolic PDE. Indian Institute of Space Science and Technology, Thiruvananthapuram. (2013).
- [19] Plamen Koev: Numerical Methods for Partial Differential Equations, Spring. (2005).
- [20] M. Thongmoon, R. McKibbin and S. Tangmanee: Numerical solution of a 3-D advection-dispersion model for pollutant transport. Thai Journal of Mathematics. **5**(1), 91-108 (2012).
- [21] Dr. H. A. Radwan, Dr. amaar Elattar, Dr. Rania khmes: Global Water Resources. Pella Conference on Water. **1**, (2010).
- [22] Suaad Hadi Hassan Al-Taai: Water pollution Its causes and effects. IOP conference series Earth and Environment Science. **790**(1), (2021), doi:10.1088/1755-1315/790/1/012026.
- [23] Zafenate Infinity: Determining the Diffusivity Coefficients for the Different NaCl Concentrations Laboratory Assignment. Report on the Liquid Diffusion Coefficient of NaCl by BSC Gumede @ UJ Department of Chemical Engineering. (2022).
- [24] Abdul-Majid Wazwaz: A comparison between Adomian decomposition method and Taylor series method in the series solutions. Applied Mathematics and Computation. **97** (1), 37-44 (1998).
- [25] Rayne of the Wine Country: Decoding your water test: Understanding water hardness and TDS levels. Rayne of the Wine Country Blog, (2025).
- [26] U.S. Geological Survey: Hardness of Water. Water Science School, U.S. Geological Survey (2018).